Chapter

Corrosion Fatigue Behavior and Damage Mechanism of the Bridge Cable Structures

Guowen Yao, Xuanbo He, Jiawei Liu, Jiangshan Lu and Zengwei Guo

Abstract

The long-term performance and corrosion fatigue damage status were investigated and analyzed under the service environment for the cable structures in cable-stayed bridges, suspension bridges, and suspender arch bridges. The artificial accelerated corrosion fatigue tests were carried out on galvanized parallel steel wire under coupled loading and environments. The damage mechanisms of galvanized parallel steel wire in corrosion, stress corrosion, and corrosion fatigue were investigated. The change laws of the mechanical properties of the cable were studied. Based on the image gray analysis, the evaluation method was proposed for the technical status of the damaged cable. Furthermore, combined with the cable damage evolution model, the service life prediction method and assessment technology of cables based on damage safety are established.

Keywords: bridge engineering, corrosion fatigue, cable structure, steel wire, damage

1. Introduction

The construction of large-span cable-stayed bridges around the world is at its peak, and a large number of cable-stayed bridges are already in the operational maintenance phase. The cable-stayed structure is one of the main load-bearing structures of cable-stayed bridges, and its durability directly affects the safety of bridge operation. As the cable system is subjected to long-term alternating loads and exposed to the natural environment, it is highly susceptible to environmental erosion. In particular, the acid rain area in China has accounted for one-third of the national territory, becoming the third largest heavy acid rain deposition area in the world after Europe and North America. In such areas with serious atmospheric pollution and water pollution or marine environment, the steel wire inside the cable-stayed bridge is highly susceptible to erosion by corrosive media, such as SO_4^{2-} and Cl^- in the environment. When the wire inside the cable breaks due to severe corrosion, it can lead to the failure of the cable system, affecting the safety and service life of the bridge, and the dangerous

situation can cause serious economic losses and safety accidents. Therefore, cable corrosion and wire breakage have become the problems faced by most cable-stayed bridges.

In this chapter, the investigation and statistical analysis of the working performance and corrosion fatigue damage of cable under service environment are carried out for cable-stayed bridges, suspension bridges, arch bridges, and other bridge cable structures, and indoor artificially accelerated corrosion fatigue test research under the coupling effect of load and environment is conducted to reveal the corrosion fatigue damage mechanism of galvanized parallel wire cable under the coupling effect of salt spray environment and static stress and alternating stress. The physical and mechanical properties of the damaged cables were studied. The technical condition assessment method based on the image grayscale analysis is established and further combined with the cable damage evolution model, the service life prediction method and assessment technology based on the breakage safety of cable are established to provide a theoretical basis for the scientific evaluation of the technical condition of cable-stayed bridges, prolonging the service life of the cable and improving the anti-corrosion design of the cable.

2. Investigation and analysis of corrosion and fatigue conditions of bridge cable structures under service environment

The survey of cable-stayed bridges built around the world shows that cable-stayed bridges are facing serious challenges and threats from cable durability issues (**Figure 1**). For example, the South Pan River Bridge in Guizhou, the original main bridge was a 240-meter span steel truss suspension bridge, which was put into operation in November 1998 and has been in operation for less than 17 years, the main cable and sling suffered from severe corrosion was dismantled in 2015 and rebuilt as a continuous rigid structure bridge. Built in 2012, the Ximo River Bridge on the county highway from Zamu Town to Murdo in Bomi County, Tibet was also facing replacement when its main cable and sling were found to be seriously corroded during an inspection in 2017. The cable of cable-stayed bridges and the suspenders of half-through and through-arch bridges are more frequently replaced due to corrosion damage and reduced reliability. The St. Nazaire Bridge in France suffered from severe corrosion during its service life, with extensive rusting and spalling of the cable

Figure 1.
Corrosion and fatigue damage of cable-stayed bridges in mountainous areas with cable-stayed cable, suspension cable, and main cable.

surfaces. After two years of operation, the Kohlbrand Estuary Bridge in Germany suffered from severe corrosion at the lower anchorage end of its cable, with 25 broken wires in the cable, and the entire bridge was replaced at the cost of $60 million or four times as much as original cost. The cost of replacing the corroded cable-stay on the Maracaibo Bridge in Venezuela is also about $50 million.

Japan and the United States have conducted experimental and theoretical studies on the corrosion of cable for a long time, especially the corrosion of cable in the marine environment. The Honshu-Shikoku Bridge Management Department in Japan has accumulated years of survey data through on-site investigations and detailed knowledge of the damage caused by corrosion of cable in several cable-stayed and suspension bridges during operation and has conducted research on preventive maintenance methods for cable, proposing measures such as anticorrosion coating coverage, ventilation, and dehumidification, as well as static and dynamic behavior monitoring [1]. Kheyroddin [2] used seawater as a corrosive medium and carried out accelerated corrosion tests under static stress to comparatively study the anticorrosion effect of different protection systems. In addition, Barton [3] focused on the corrosion behavior of lasso in NaCl corrosive medium by artificially accelerated corrosion experiment, obtaining the weight loss of steel wire samples, hydrogen concentration, elongation, etc. The results of the study showed that water and temperature are the environmental factors most likely to cause corrosion of lasso, and accelerated corrosion test proves that the most serious corrosion occurs at the anchored end of lasso, the middle and the top end is less affected by corrosion, and the increase of NaCl concentration in the solution and temperature will accelerate the corrosion process of galvanized steel strands. In 1987, Dolley [4] and Mahmoud [5] surveyed nearly 100 cable-stayed bridges around the world and conducted a visual inspection of the bridges, finding that "nearly 200 cable-stayed bridges built worldwide in the last few decades are at risk due to cable corrosion." The new parallel wire system that was introduced in Japan also has a corrosion resistance life of only 25–30 years. Cable-stayed bridges are experiencing serious challenges and threats from cable durability issues [6–10].

3. Artificially accelerated corrosion fatigue experiment under coupled loading and environment

3.1 Experiment content and its implementation

Accelerated corrosion experiment was conducted on lassos using an acidic salt spray environment. The cable consisted of high-strength galvanized parallel steel wire. The strength level of the lasso is 1860 MPa, the yield strength is 1660 MPa, and the diameter φ is 5.2 mm. The loading force for both alternating stress and static stress is 1100 MPa, which is close to the stress corrosion threshold. At the end of the experiment, the steel wire was wiped with 10% dilute sulfuric acid to remove the surface corrosion, the mass loss of the steel wire subjected to corrosion was measured, and the mechanical properties of the corroded steel wire were tested to discuss the mechanical property response of the steel wire to the corrosive environment and to provide an experimental data basis for evaluating the corrosion damage and evolution of the steel wire. The main experimental equipment is shown in **Table 1**.

The salt solution was 5% NaCl solution, adding concentrated sulfuric acid in the solution to adjust the pH to 1. The experiment temperature reference document [11]

Name	Model	Technical parameters	Quantity (units)
Salt spray test chamber	YC-200	Salt spray deposition: 250 ml/m^2/h	1
Electro-hydraulic servo universal testing machine	WAW-1000	Maximum load: 1000 kN	1
Electronic balance	SL500ZN	Precision: 0.01 g	1
Double-acting hollow jack	ZKD	Carrying capacity: 20 t	4
Ultra-high-pressure electric oil pump	DSS	Power: 0.75 kW	1

Table 1.
Main experimental equipment.

will be set at 50°C ± 2°C, the air pressure is controlled between 70–170 kPa. Spray volume reference document [11] CASS experimental standards, taken as 250 ml/m^2/h. The specific implementation steps of experiment are as follows: All the treated steel wire were weighed with a balance, the diameters were measured, and the raw data were recorded. The experiment was arranged in three loading methods: stress-free, static stress, and alternating stress. The stress-free loading method cut the steel wire into 1.2 m sections, marked them, and put them directly into the corrosion chamber for continuous corrosion without interruption. When subjected to static stress loading, the steel wire is cut into 5.4 m sections, marked and through the corrosion box and the counter-weight table reserved hole, and anchored with a tensioning jack, the rest of the process is same as stress-free loading. Alternating stress loading, the same steel wire is cut into 5.4 m sections, the loading cycle for 4 h, that is, 2 h loading, 2 h unloading, the rest of the work is same as stress-free loading, every 24 h to open the corrosion box, take pictures, and record data, reconfigure and add solution. After the experiment, first, clean the corrosion products on the specimen with dilute sulfuric acid, then wash the steel wire with a large amount of water, blow dry with a blowing air and then weigh again, the diameter should be randomly measured three times for each specimen section, and take its average value and record. The last is the corrosion of steel wire mechanical tensile experiment.

In this experiment, at least five steel wires were used in each batch, two of which were alternately stressed, two were statically stressed, and the others were unstressed wires. The peak stress applied is 1100 MPa. The specific arrangement is shown in **Figure 2** [12].

Before conducting the formal tensile experiment, three intact steel wire samples with a length of 1 m were taken and tensile experiments were performed on them with a universal testing machine. Their elastic modulus E, tensile strength R_m, yield strength $R_{p0.2,}$ and post-break elongation A were measured to determine the original mechanical properties parameters of the steel wire. It provides a reference for the test results of mechanical properties of steel wire after corrosion. The data obtained from the tensile experiment are given in **Table 2**.

In order to ensure the safety of the bridges, considering the safety factor of the steel wire used in cable-stayed bridges, the stresses applied during their operation should be less than their yield strength and tensile strength. Therefore, it is reasonable to apply a maximum tensile stress of 1100 MPa to the galvanized steel wire to ensure that they do not yield and fracture during the experimental process.

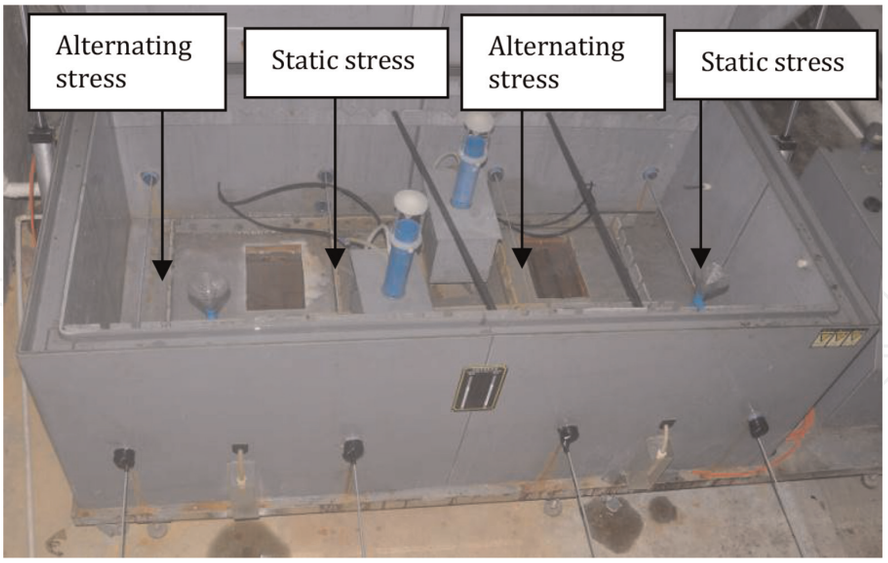

Figure 2.
Experimental specimen arrangement.

Number	E (GPa)	R_m (MPa)	$R_{p0.2}$ (MPa)	A (%)
1	205.54	1915	1760	5.5
2	231.36	1910	1710	6.0
3	213.20	1910	1730	4.5

Table 2.
Steel wire static performance experiment data.

3.2 Steel wire corrosion fatigue damage phenomenon

After the test of each batch of steel wire specimens placed in the corrosion test chamber, take them out to observe the morphology of corrosion products, and then remove the corrosion products. Wait for the drying of the steel wire and then observe its surface morphology, and preliminarily analyze the experimental phenomenon (**Figure 3**) [13], the conclusions are as follows:

1. Under the erosion of the corrosion solution, the corrosive medium in the solution gradually accumulates on the surface of the galvanized layer of the steel wire, and the galvanized layer undergoes nonuniform corrosion and gradually produces corrosion pits. The acidic corrosion solution penetrates into the corrosion pits, which continue to develop in depth and appear white corrosion, with the main corrosion product being $Zn(OH)_2$-$3ZnSO_4$–$5H_2O$. Due to stress, cracks appear in the galvanized layer of the steel wire surface, corrosion pits continue to expand and increase, the surface damage is further aggravated, the corrosive medium is more likely to penetrate into the galvanized layer, and the degree of corrosion of the steel wire continues to increase, which led to a large diameter of the corrosion pit on the surface of the steel wire. (**Figure 3a**);

2. With the further development of corrosion, white corrosion increases, and red corrosion is seen sporadically in the galvanized layer corrosion products. The area

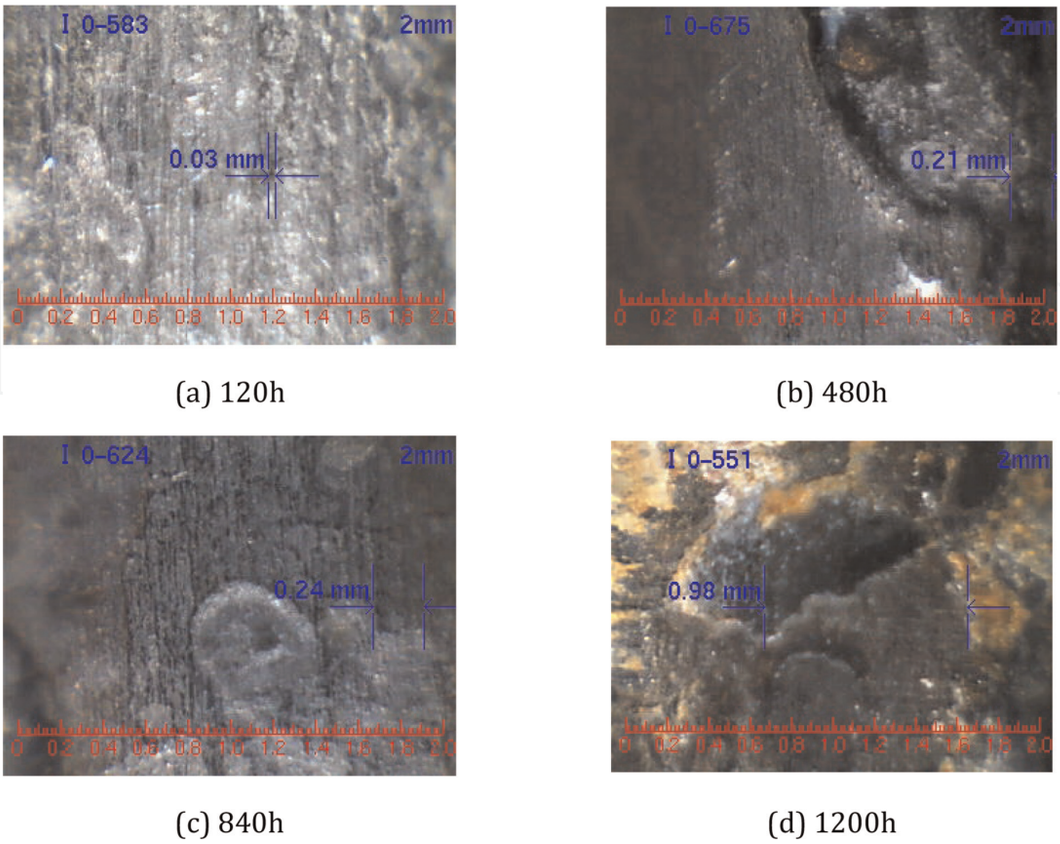

Figure 3.
Apparent condition of steel wire with different corrosion times [13] (a) 120 h (b) 480 h (c) 840 h (d) 1200 h.

and depth of the corrosion pits increase. After removing the corrosion products, the galvanized layer was covered with black oxide at the location of the corrosion pits, whose composition was mainly $Fe(OH)_3$, Fe_2O_3–H_2O and $Fe_2(SO_4)_3$–$8H_2O$. The surface of the steel wire in the uncorroded area around the corrosion pit is still relatively bright, and the degree of corrosion of the steel wire is relatively mild. Through these phenomena, it can be proved that the corrosion type of galvanized steel wire is anodic dissolution type, in which the exposed iron matrix reacts electrochemically with the surrounding corrosion products and H^+ is reduced to atomic hydrogen, and gradually migrates to the deeper layer of the matrix through concentration diffusion (**Figure 3b**).

3. When the galvanized layer is exhausted, the white corrosion product disappears and is replaced by a larger area of red corrosion, and the entire surface of the steel wire is no longer shiny after the corrosion product is removed. The expansion of some corrosion pits becomes slow or even stops expanding. At this point, many corrosion pits begin to fuse with each other, linked together into larger corrosion pits or grooves, whose depth of color is shallow. Due to the merging of small corrosion pits, the number of corrosion pits is significantly reduced (**Figure 3c**).

4. In the late stage of corrosion, red corrosion has completely covered the surface of the steel wire, and after removing the corrosion products, a large amount of iron matrix can be found leaking out, and the surface of the whole steel wire has a naked-eye visible unevenness, and corrosion has occurred in almost all areas to varying degrees (**Figure 3d**).

3.3 Steel wire corrosion fatigue loss of weight

In order to facilitate data processing, the problem of uneven distribution of steel wire density along the axial direction is ignored, and the weight of the steel wire is converted to unit length weight. And use the same method to deal with the corrosion of the steel wire, the data of weight loss over time before and after corrosion are recorded separately (**Table 3**) [14]. The table shows the weight W_1 before corrosion, weight W_2 after corrosion, weightlessness W_3, diameter D_1 after corrosion, average diameter $D_{2,}$ and corrosion time H.

It can be seen from the experimental data, the weight of the steel wire is reduced over time in the experiment, and the growing trend of different stress states of the steel wire is basically the same. In the three stress states, although the weight loss per unit area at a particular moment is not very regular, according to their respective trends to analyze, the overall still follow such a law: In any stage of corrosion of the steel wire, the stress complex steel wire in a corrosive environment is more vulnerable to corrosion.

H (h)	Number	Loading method	W_1 (g/m)	W_2 (g/m)	W_3 (g/m^2)	D_1 (mm)	D_2 (mm)
120	1	Alternating stress	166.8	164.8	125.1	5.23	5.23
	2	Static stress	167.1	165.4	102.2	5.23	
	3	Stress-free	166.7	165.3	86.1	5.23	
240	1	Alternating stress	167.1	163.3	234.1	5.18	5.19
	2	Alternating stress	167.1	163.7	208.2	5.18	
	3	Static stress	167.1	164.8	141.5	5.18	
	4	Static stress	167.0	164.2	171.4	5.20	
	5	Stress-free	167.1	164.8	137.4	5.19	
360	1	Stress-free	166.7	163.3	209.1	5.20	5.20
480	1	Alternating stress	166.9	162.5	271.0	5.17	5.18
	2	Static stress	166.9	162.6	263.2	5.18	
	3	Stress-free	166.6	162.4	257.3	5.18	
840	1	Alternating stress	166.8	160.8	367.5	5.14	5.18
	2	Static stress	167.4	161.9	334.1	5.20	
	3	Stress-free	166.8	161.7	316.8	5.20	
	4	Stress-free	166.9	161.8	313.0	5.16	
1200	1	Alternating stress	167.0	159.9	434.6	5.11	5.16
	2	Static stress	167.2	161.0	379.0	5.14	
	3	Stress-free	167.2	161.6	344.3	5.19	
	4	Stress-free	167.1	161.5	340.6	5.18	
1560	1	Stress-free	166.7	159.3	448.9	5.14	5.13
	2	Stress-free	166.9	159.6	446.3	5.12	
	3	Stress-free	166.6	157.8	539.6	5.12	

Table 3.
Steel wire corrosion fatigue loss of weight date [14].

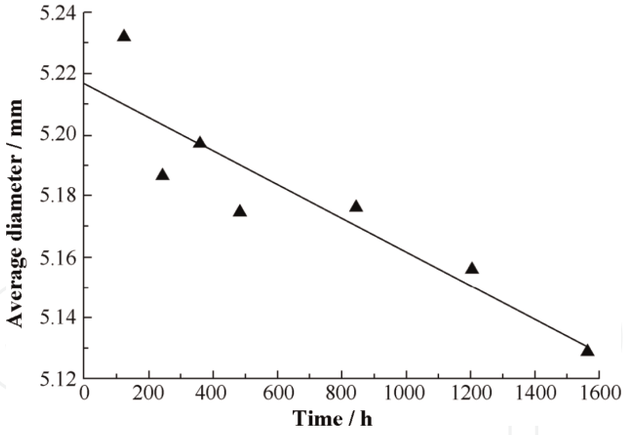

Figure 4.
Relationship between corrosion time and average diameter of each group [13].

Considering the fatigue effect of the wire, alternating stress is not only easy to cause fatigue damage to the steel wire but also may accelerate the chemical corrosion of its surface in a corrosive environment, causing a decrease in the cross-sectional area of steel wire, increasing the stress on the steel wire, and reducing the safety factor of the cable.

Without considering the stress state of the steel wire, the relationship between the diameter of the corroded steel wire and time is plotted in **Figure 4**.

As can be seen from **Figure 4**, the trend of decreasing the diameter of corroded steel wire is linear. The corrosion time is 5 days, and the diameter of the steel wire is 5.23 mm, greater than the standard diameter of the steel wire 5.2 mm, which is due to the fact that the zinc layer thickness will be slightly higher than the specified value in order to protect the quality of the steel wire [13]. The actual experimental wire diameter before corrosion is between 5.23 mm and 5.25 mm, and the effect of 5 days of corrosion on the diameter is not significant, measured with a micrometer will also produce a certain error.

4. Corrosion fatigue damage mechanism and damage evolution model of galvanized parallel steel wire

4.1 Steel wire mesoscopic view analysis based on image grayscale

In order to obtain a quantitative evaluation index, the corrosion degree of the steel wire is evaluated by a gray image-based method to calculate the corrosion pit density of the steel wire, and the degree of corrosion is defined by the percentage of corrosion pit density. Use GSA image analyzer software to perform grayscale analysis of eroded images. GSA Image Analyzer is an image analysis tool that supports all types of 2D images with comprehensive functions to identify and count the number of objects; supports length and area calculation; supports patterns from files, scanners, and microscopes; and can be used in fields such as cell analysis and materials engineering. Since the image formed by the electron beam scanning of the corroded steel wire is a true color image and cannot be recognized directly on the computer, it is digitized and converted into a grayscale image using GSA Image Analyzer. The principle of digital processing is to convert a true-color image into an array of pixels that can be represented numerically, with the value of each dot being the grayscale value of that dot. The spatial resolution of the original image is related to the number of pixel dots there are, the more dots, the higher the pixel resolution is.

With the increase in corrosion time, the local adjacent corrosion pits interlocked, forming larger corrosion pits, and the corrosion pit depth also gradually increased. Under the alternating stress condition and static stress condition, the stress in the pitting area is concentrated and cracks are gradually formed and expanded. The selected corroded wire is cleaned to ensure no residue and then dried in the drying oven. For observation, the dried steel wire was placed on the sample plate to sketch the position, then the sample plate was placed in the sample chamber, the sample chamber was sealed, and the steel wire was observed under the electron microscope. As an example, **Figures 5** and **6** [15, 16] show the microcracking phenomenon on the steel wire surface under alternating stress and static stress conditions.

According to **Figures 5** and **6**, it can be seen that the depth and size of the corrosion pits are gradually developed with the corrosion process. Under the coupling effect of stress and corrosive environment, the nucleation of the corrosion pits of the corroded steel wire is first cracked and forms nanoscale cracks, while the alternating stress makes the nanoscale cracks continuously elongate and retract, resulting in the accelerated formation of microcracks in the steel wire.

As shown in **Figure 7** [17], the local corrosion map of 300 times under each working condition was imported, and the hue was measured at the parts where the steel wire corrosion was obvious, and the histogram of the hue distribution was derived and the distribution amount was counted to calculate the frequency of corrosion pits. After the numerical processing, combined with the distribution histogram to obtain the corrosion characteristics of the specimen surface parameters can be seen that the corrosion

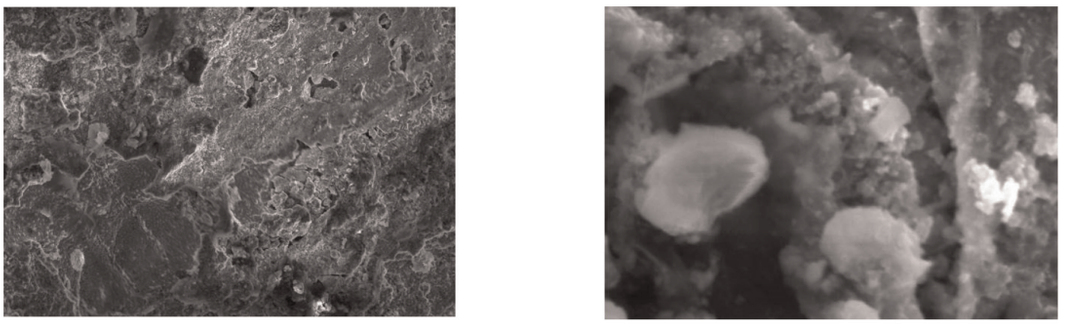

(a) 300 times (b) 6000 times

Figure 5.
Alternating stress microcrack extension [15, 16] (a) 300 times (b) 6000 times.

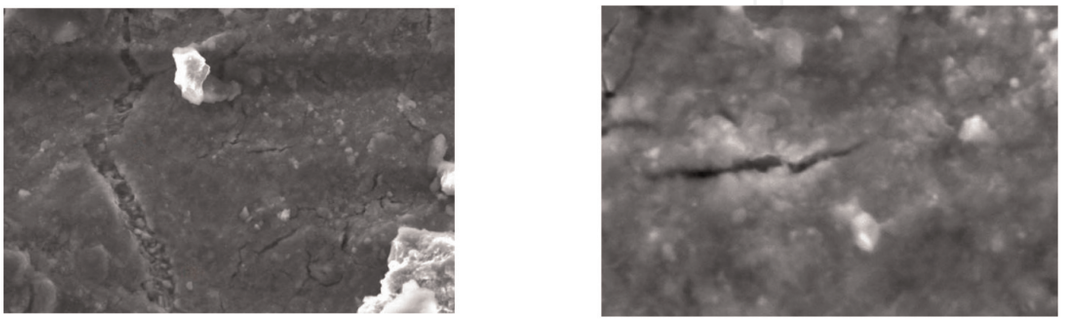

(a) 1380 times (b) 6000 times

Figure 6.
Static stress microcrack extension [15, 16] (a) 1380 times (b) 6000 times.

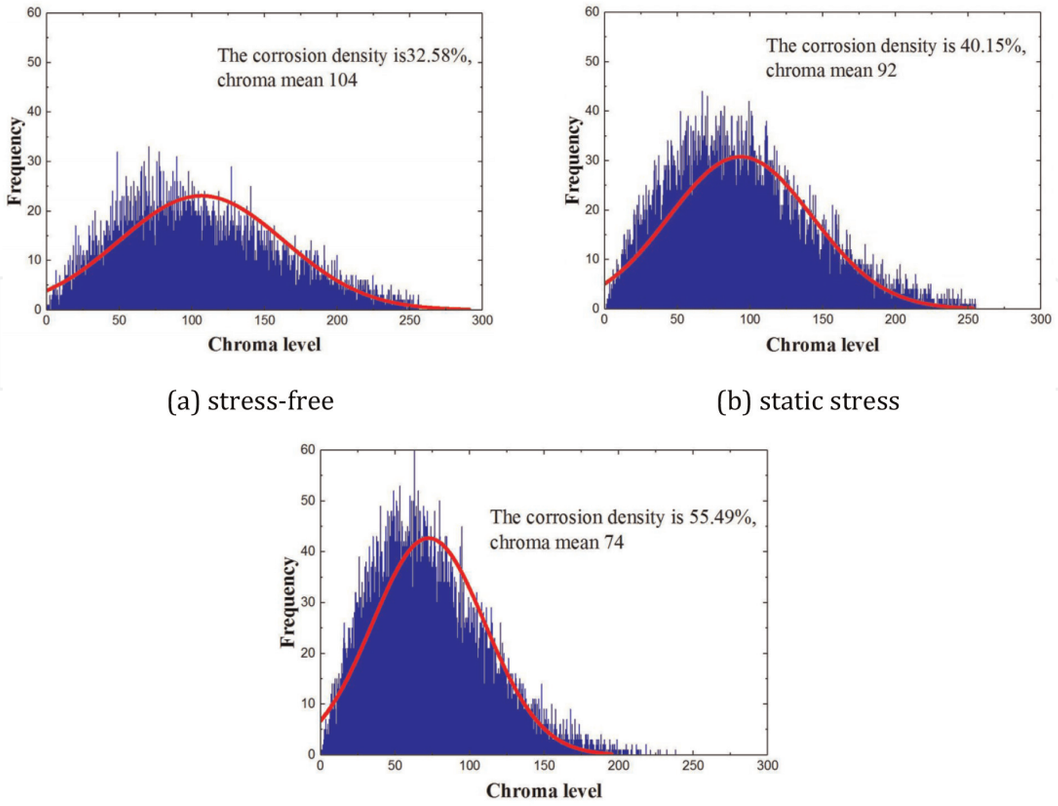

(a) stress-free

(b) static stress

(c) alternating stress

Figure 7.
Corrosion histogram [17] (a) stress-free, (b) static stress, and (c) alternating stress.

characteristics of the steel wire basically conform to the normal distribution. In the salt spray environment under stress-free conditions, there is no obvious corrosion pit in the specimen and the corrosion rate is about 32.58%. The corrosion rate under alternating stress conditions is about 55.49%. Under the static stress condition, the corrosion rate of steel wire is between the previous two conditions, about 40.12%. Wire corrosion is more uniform under stress-free conditions, and the standard deviation of its histogram is larger, with a color tone level of about 104, while the color tone level of the peak gray standard deviation of the static stress condition is about 92, which is between the alternating stress condition and the stress-free condition. For the alternating stress condition, the steel wire surface tone value concentration and corrosion pits with the elongation and retraction of the steel wire to accelerate the development of the peak where the tone level is about 74. Therefore, under the alternating stress condition, the corrosion frequency and corrosion rate of the steel wire are greater than the rest of the conditions, and the damage to the specimen is the largest.

4.2 The mechanical property analysis of corroded steel wire

The corroded steel wire was stretched in one direction on the universal testing machine, and its mechanical property data were recorded, and the broken steel wire of each steel wire was packed and numbered after completion. Select the middle length of the steel wires as a 1-meter section of the experimental section for tensile experiments, the ratio of the maximum load measured before the experimental section is

H (h)	Number	E (GPa)	AVG	R_m (MPa)	AVG	$R_{p0.2}$ (MPa)	AVG	A (%)	AVG
120	1	209.7	212.0	1890	1890	1615	1653	6.5	5.5
	2	210.2		1880		1625		5.5	
	3	216.0		1900		1720		4.5	
240	1	208.2	213.0	1905	1902	1610	1636	5.0	4.6
	2	208.7		1905		1625		2.0	
	3	214.1		1900		1610		4.5	
	4	216.2		1895		1620		5.5	
	5	217.8		1905		1715		6.0	
360	1	213.3	213.3	1900	1900	1730	1730	5.0	5.0
480	1	226.0	229.3	1900	1897	1595	1623	4.5	4.7
	2	303.8		1905		1585		5.0	
	3	232.7		1885		1690		4.5	
840	1	222.6	216.0	1880	1868	1585	1656	5.0	4.5
	2	214.8		1865		1650		4.5	
	3	215.8		1865		1690		4.5	
	4	211.0		1860		1700		4.0	
1200	1	184.8	206.9	1905	1883		1690	2.0	4.0
	2	214.2		1895		1690		5.5	
	3	209.4		1860		1685		4.0	
	4	219.2		1870		1695		4.5	
1560	1	208.8	208.9	1825	1802	1670	1653	3.5	3.0
	2	209.5		1815		1655		3.0	
	3	208.4		1765		1635		2.5	

Table 4.
Mechanical property data of steel wire.

pulled off and its nominal area is the tensile strength, that is, the nominal tensile strength. The mechanical property data are shown in **Table 4**.

According to the analysis of the changes in the mechanical properties data of the steel wire in **Table 4**, it can be seen as follows:

1. The stress state of the steel wire after corrosion is different, its elastic modulus and yield strength vary less, and only the elongation differs significantly through preliminary analysis. Since the corrosion loss weight obtained in the previous article is linearly related to time, the alternating stress, static stress, and stress-free loading state of the specimen elastic modulus with corrosion time change is not significant, the elastic modulus of corrosion is also not sensitive to corrosion performance;

2. In the early stage of corrosion, stress corrosion and corrosion fatigue have little effect on tensile strength, the tensile strength between the three loading states is not significantly different, and the size of the tensile strength has not decreased significantly;

3. In the middle and late stages of corrosion, the tensile strength began to decline sharply. Alternating stress-loaded specimens and static stress-loaded specimens will show a brief increase in tensile strength. This is a hazardous increase and should be given sufficient attention. The decrease in steel wire ductility can be reflected from the side;

4. According to the document in Ref. [18], the post-break elongation of 1860-grade galvanized steel wire shall not be less than 4.0%. And in the late stage of corrosion, the post-break elongation of the three loading states of the steel wire dropped below 4.0%;

5. In the late stage of corrosion, the alternating stress loading causes corrosion fatigue damage to the cable, and its post-break elongation was significantly lower than that of the other two loading modes of the steel wire, which indicates that the alternating load reduced the toughness of the steel wire.

In summary, the mechanical property of the specimens under different loading states was affected to different degrees by the prolongation of corrosion time, and the modulus of elasticity, yield strength, tensile strength, and elongation after fracture all showed a downward trend. Among them, tensile strength and elongation after a break are the most sensitive to corrosion, while the modulus of elasticity is less sensitive to corrosion, tensile strength decreases slowly in the early stage of corrosion, and in the middle and late stages, it decreases in a leap and becomes more sensitive to corrosion, the different loading methods have a greater impact on the yield strength.

4.3 Corroded steel wire fracture morphology analysis

In the static tensile experiment of uncorroded steel wire, it was found that the fracture form is mainly manifested as cup-cone, the fracture form of specimens under stress-free conditions is also a cup-cone fracture (**Figure 8a**), but not as regular as the fracture of uncorroded specimens, the fracture form of specimens under static stress conditions is mainly milling cutter fracture (**Figure 8b**), individual specimen is cup-cone fracture, the fracture form of specimens under alternating stress conditions is mainly cleavage-milled fracture (**Figure 8c**), individual steel wire is miter-type fracture and their combined form, but there are very few cleavage fractures (**Figure 8d**) [15].

From **Figures 8a** and **b**, it can be seen that the cup-cone fracture has an obvious necking phenomenon, the milling cutter fracture also has the appearance of necking but not as obvious as the cup-cone fracture, this necking phenomenon indicates that the steel wire material has obvious plastic properties; while **Figure 8c** and **d**, there is no obvious necking phenomenon in cleavage fracture and cleavage-milled fracture, which shows the brittle properties of steel wire material, and the fracture time and location performance, the fracture time and location are sudden and uncertain. The probability of brittle fracture of the steel wire is the highest under the action of alternating stress and environmental coupling, corrosion fatigue is usually multisource fatigue, the fracture has more fuzzy fatigue striations or brittle fatigue cracks, and there are more secondary cracks in the fracture.

After the mechanical properties experiment on the corroded steel wire, the fracture of the corroded steel wire under alternating stress conditions was scanned with KYKY-2008B digital scanning electron microscope, and the microscopic morphology of the fracture is shown in **Figure 9a–d** [15].

DOI: http://dx.doi.org/10.5772/intechopen.109105

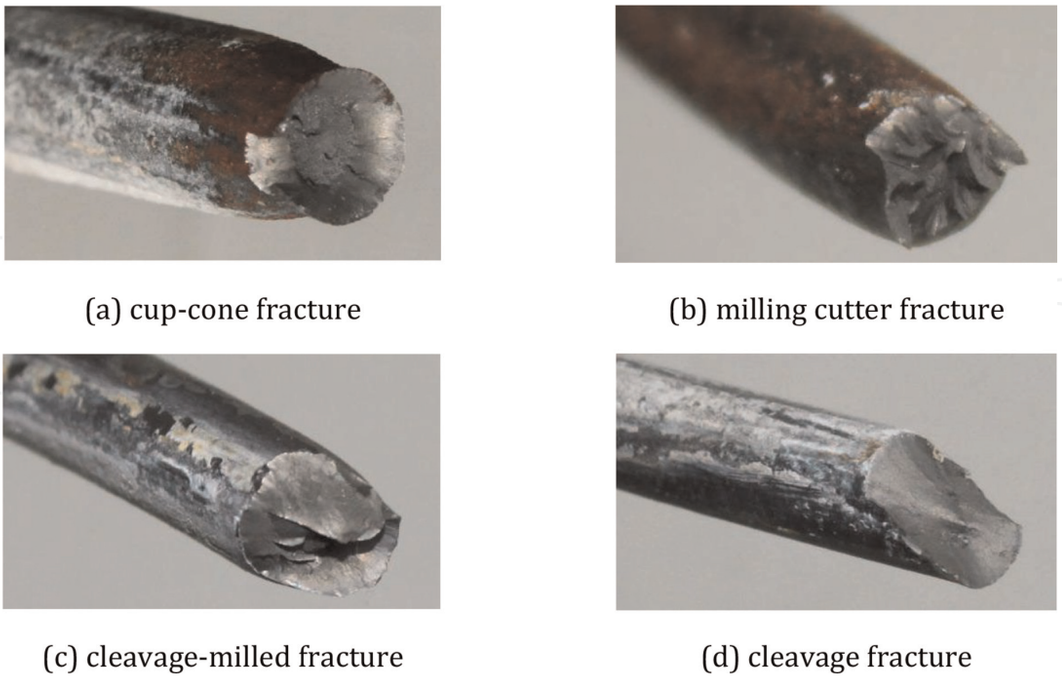

Figure 8.
Fracture morphology of corroded steel wire under different stress conditions [15] (a) cup-cone fracture, (b) milling cutter fracture, and (c) cleavage-milled fracture (d) cleavage fracture.

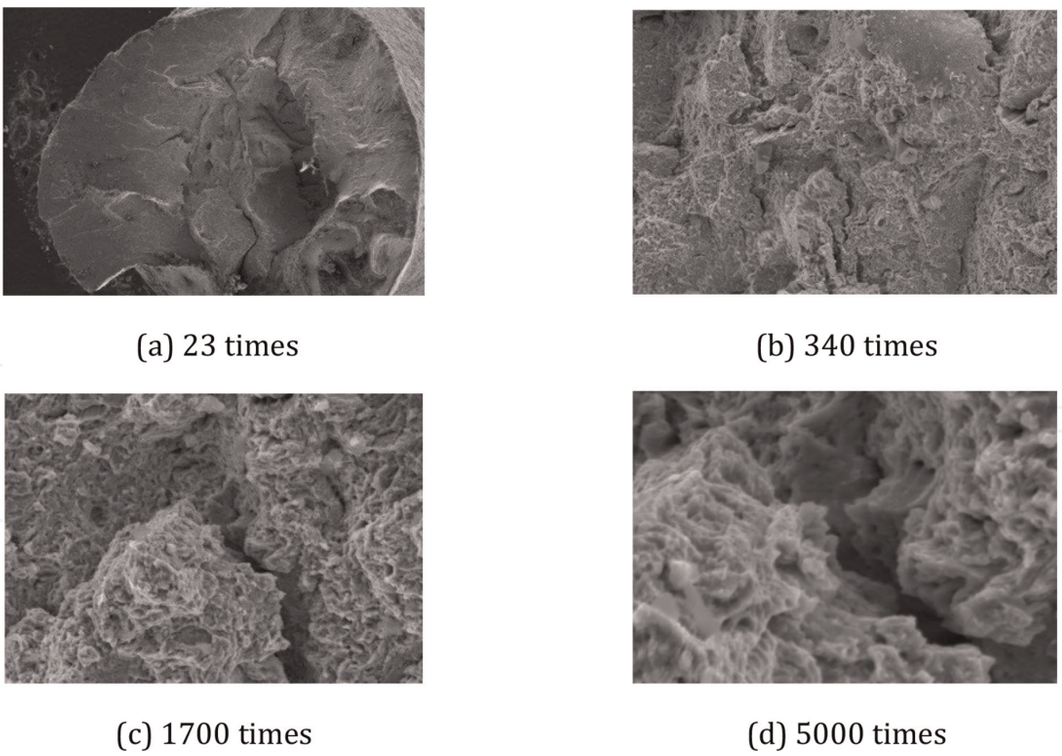

Figure 9.
Morphology of the fracture under alternating stress [15] (a) 23 times, (b) 340 times, (c) 1700 times, and (d) 5000 times.

After magnification, it can be found that a few sections of the edge of the fracture are neat and show a brittle fracture morphology, while other areas are destructive in shape, and individual areas appear in a river and mountain-like morphology. The

center of the fracture appears to have a tough nest-like morphology. When the fracture is magnified to 1700 times by microscope, a "fish-eye" morphology can be seen, and a shell-like fracture appears. This morphology is caused by fatigue, which indicates that the fracture is controlled by the main crack and gradually expands along the expansion of the main crack. As the primary crack grew and expanded, the secondary crack also expanded gradually, which accelerates the fracture of the steel wire. When the fracture is magnified to 5000 times by microscope, a large number of smooth "fish eye" shapes are distributed on the section, according to the shape of the fracture, it can be seen that corrosion of the steel wire is a brittle fracture. The experiment shows that corrosion of severe steel wire plastic properties reduced, brittly enhanced, and the time of fracture is uncertain, with abruptness under the alternating stress and environmental coupling.

5. Working life prediction method and evaluation technology for cable based on breakage safety

5.1 Working life prediction method of service cable

Based on the experimental analysis, compared with non-corroded steel wire, the pitting corrosion, fracture stress, and elongation after fracture of corroded steel wire in the nucleation stage are basically unchanged, the remaining life prediction of this stage is not considered. The process of corrosion pits growing and expanding until they turn into small cracks is a common stage of the steel wire in service cable. At this stage, the life of the steel wire is reduced. After the appearance of the crack, the corrosive environment and the coupling of alternating stresses made the expansion rate of the crack rapidly increase to the maximum, breaking stress and elongation after fracture are sharply reduced, the steel wire toughness is reduced, and brittleness enhanced, there is a turn from tough to brittle at this stage [19]. In order to prevent the appearance of brittle fracture, the steel wire of the cable needs to be avoided in this stage of work, the critical crack appears, and the steel wire brittle fracture will occur at any time, the study of its life is also not considered. Therefore, the reliability of the steel wire of the service cable is affected by the development of corrosion pits until the appearance of small cracks and the appearance of small cracks until the appearance of the critical crack size a_c [15].

The law of fatigue crack expansion can be used to analyze the reliability of in-service ties as well as risk of safety. The fatigue crack expansion rate function commonly used in engineering is the Paris-Erdogan model, that is, the Paris formula, which establishes the relationship between the stress intensity factor and the crack expansion rate and is the theoretical basis for predicting the fatigue crack expansion life in the form shown in Eq. (1):

$$da/dN = C(\Delta K)^n \tag{1}$$

where a is the crack length; N is the number of stress cycles; da/dN is the crack expansion rate; C, n is the material constant, environmental factors such as temperature, humidity, media, loading frequency, etc. are obtained by fitting the experimental data.

ΔK is the stress intensity factor amplitude and is described by Eq. (2):

$$\Delta K = K_{max} - K_{min} = f\Delta\sigma\sqrt{\pi a} \tag{2}$$

where f is a function of member geometry and crack size; K_{max} and K_{min} are the maximum and minimum values of the stress intensity factor at the crack; and $\Delta\sigma$ is the stress amplitude at the crack.

At the stage in which corrosion pits develop into small cracks, each growth of initial defect is independent, the growth of corrosion pit is slow and also affected by accumulation of corrosion product and other factors. while in the small crack until the critical crack size a_c stage, the growth of crack depth is faster, the growth rate increased rapidly to the maximum, the expansion rate is significantly greater than the previous stage.

On the basis of the Paris formula, the corrosion fatigue calculation is simplified into two linear stages, namely, the life of the corrosion pit development to the crack stage N_1 and the life of the tough and brittle expansion stage N_2, the total life of the wire of the cable is equal to the sum of life of these two stages, expansion of corrosion fatigue crack generally meets the deformation form of Paris formula, as shown in Eq. (3):

$$da/dN = D(t)(\Delta K)^m \tag{3}$$

where m is the material constant, generally close to the parameter m in simple fatigue; $D(t)$ is related to the material medium system, loading frequency and load form and other factors, and is a function about time t, instead of the original constant c.

In a comprehensive analysis, the key to applying this method is to determine the range of different stress intensity factors ΔK, the initial corrosion pit size a_0, the initial crack size a_f, and the critical crack size a_c for these two segments. based on this, the life of each stage and the total life N are described by Eqs. (4) to (6).

$$N_1 = \int_{a_0}^{a_f} da \Big/ \left[\frac{da}{dN}\right]_1 \tag{4}$$

$$N_2 = \int_{a_f}^{a_c} da \Big/ \left[\frac{da}{dN}\right]_2 \tag{5}$$

$$N = N_1 + N_2 \tag{6}$$

5.2 Safety assessment of damage cable

Cable may fail in two ways after experiencing long-term accumulated damage: One way is that the damage makes the cable reach the critical state that is unsuitable for use and even makes the cable fail under the action of conventional load; another way is that the accumulated damage causes the cable resistance to decay. By now, although the damage does not reach the critical value, part of the steel wire or even the whole cable may suddenly fail when the lasso encounters the action of accidental extreme load. Therefore, it is necessary to effectively detect, monitor, and predict the process of damage accumulation of the cable, grasp the law that its resistance decay with the accumulation of damage, and timely repair and reinforce cable to ensure the safe operation of the cable structure and avoid the occurrence of accidents to the maximum extent possible [19–22].

(1) Evaluation of steel wire corrosion based on appearance: Relying on a unified hard and fast objective standard, so that each tester is bound by this standard and does not rely entirely on subjective guesses to draw conclusions.

(2) Assessment of effective strength reduction factor based on appearance quality: Usually based on the experimental analysis of some representative bridge cables, the empirical formula for regression analysis of cable's strength is used to assess the safety of cables or investigate the influence of defects and diseases of a large number of bridge cables on the bearing capacity of the bridge, determine a more reasonable strength reduction factor according to the investigation results, and then discount the strength of the cable. In this method, the effective resistance of the damaged cable is reduced, and the actual resistance of the damaged cable is equal to the standard value of the steel wire tensile strength of the cable multiplied by the strength reduction factor. The calculation formula is shown in Eq. (7):

$$R^{\tau} = vR^{b} \tag{7}$$

where R^{τ} is the estimated actual tensile strength of the damaged cable, R_b is the design tensile strength value of the cable, and v is the strength reduction factor of the damaged cable.

(3) Safety assessment of cable strength based on the overall level of load effect: A detailed appearance survey is carried out for the cable, and the cable is classified according to the results of appearance survey, and its resistance calculation coefficient is determined according to the classification. The corresponding calculation coefficient Z_1 value is based on a large number of engineering accumulation and experimental statistics. Based on the detailed appearance investigation of the cable, the value of Z_1 can be referred to **Table 5**. The safety assessment of the cable based on the overall level of load effect is to judge the safety condition of the cable by comparing the relationship between the magnitude of the load effect and the resistance of the cable. Z_1 is used as the reduction factor of the resistance of the cable when calculating the resistance of the cable, and the actually allowable resistance of the cable can be calculated by Eq. (8):

$$[R]^{\tau} = Z_1 g[R]^{d} \tag{8}$$

Z_1	Technical status	Status of cable
1.00–1.10	Excellent	Complete surface protection, no water accumulation in the anchor head, and no cracks in the anchorage area.
0.95–1.00	Good	The surface protection is basically intact, with minor cracks, no corrosion of the anchor head, and no cracks in the anchorage area.
0.90–0.95	Moderate	Surface protection with a few cracks, accompanied by a few most corrosion, slight corrosion of the anchor head, and small cracks in the anchorage area.
0.85–0.90	Poor	The protection of surface is generally cracked and partially detached, the anchor head is corroded, and there are obvious stress cracks in the anchorage area.
Below 0.85	Dangerous	The protection of surface is generally cracked and has a lot of shedding, the cable is exposed and rusted severely, and the anchor head is waterlogged and corroded, there are obvious stress cracks in the anchorage area and the width is greater than 0.2 mm

Table 5.
Values of Z_1 *discount factor for cable resistance.*

where $[R]^d$ is the designed value of the cables' resistance and Z_1 is the reduction factor of the cables' resistance.

(4) Method that evaluates identification factor based on safety factor: For the safety evaluation of cable, the identification factor method from abroad can be used. In the design stage of cable-stayed bridges, a certain safety factor is usually taken for the design resistance of the cable, considering various factors such as material safety, load impact effect, and cable fatigue. The safety factor is defined as the ratio of the load effect to the resistance effect of the cable. Comparing the actual safety factor with the design safety factor, according to the design requirements, if $\eta > [\eta]$, it means that the cable is in a safe state; if $\eta = [\eta]$, it means that the cable is in a safe critical state; if $\eta < [\eta]$, the smaller the measured safety factor η the less safe the cable is under stress. The specific calculation method is shown in Eq. (9):

$$\eta = R/S \tag{9}$$

where η is the safety factor calculated by the actual measurement of the cable, R is the force of cable generated by the load effect, and S is the actual ultimate resistance of the cable.

(5) Assessment methods based on reliability theory: Safety after damage is an important indicator to evaluate the actual working performance of cable-stayed bridges in service. However, due to the differences in the working environment of the structure and the materials themselves, such as geometric characteristics, mechanical properties of the materials, load rating and distribution, and other parameters cannot be unified in the safety assessment of cableways, making the safety assessment of damaged cables uncertain. The assessment method of probabilistic reliability defines this uncertainty as a random variable to achieve the assessment of cable safety. According to the current unified standards for the design and definition of structural reliability of buildings, structural reliability is expressed as the probability that the structure will complete its intended function within a scheduled time and under specified conditions. For the cable, the safety function of the strength is first established as shown in Eq. (10):

$$Z = r - s \tag{10}$$

where s is the ultimate or design strength of the cables and r is the measured or estimated strength of the cables corresponding to s.

Since both r and S are random variables, Z is also a random variable. When $Z > 0$, the structure is in a reliable state; when $Z = 0$, the structure reaches the limit state; and when $Z < 0$, the structure is in a failure state. The static model of reliability analysis is applicable to the resistance of the structure, which hardly changes with time in the process of use, so the resistance can be regarded as a constant value. For real structures, on the other hand, the structural resistance is constantly changing over time, so the resistance of the existing structure must be simulated using a stochastic process. Assuming that the probability density function of Z is $f(Z)$, the general representation of the component safety probability calculation formula is Eq. (11).

$$R = P(Z > 0) = \int_0^\infty f(Z)dZ \tag{11}$$

The key to the safety assessment of cable strength using the reliability method is to establish the functional function and determine the distribution parameter. The

general functional functions are divided into two types, one is based on the functional function of cable resistance and another is based on the safety factor. The structural resistance and load effects in the functional functions generally obey normal distribution, lognormal distribution, and Weibull distribution. The relevant research results suggest that for generally engineering design, it is reasonable and biased toward safety to use normal distribution for member resistance and load effects. For members with high safety requirements, lognormal or two-parameter Weibull distributions are recommended.

(6) Fatigue-based safety assessment of cable: For the safety analysis of fatigue strength of cable, the Palmgren-Miner linear cumulative damage theory is commonly used in engineering, and the corresponding stress-fatigue life curve is statistically analyzed and summarized through the steel wire fatigue experiment, form a standard for the service life of cables under different load cycles, which is used to predict and evaluate the fatigue safety performance of cable.

6. Conclusions

In this chapter, through the corrosion fatigue experiment on the steel wire of bridge cable under the action of coupled environment and load explore the fine morphology of the steel wire under different corrosion time and different stress loading, analyze the law of evolution of mechanical property and the different fracture morphology of the steel wire, and analyze and generalize the service life and damage assessment technology of the cable based on the breakage safety theory, the main conclusions are as follows.

As the steel wire of the cable undergoes electrochemical reaction during corrosion, the surface of the steel wire produces white corrosion products. As the corrosion deepens, the galvanized layer on the surface of the steel wire is depleted, the white corrosion products disappear and are replaced by a larger area of red corrosion, and the surface of the entire steel wire appears uneven as visible to the naked eye.

The corrosion characteristics of the steel wire are basically in line with the normal distribution, in the salt spray environment, the steel wire did not appear obvious corrosion pits under stress-free conditions, the corrosion rate is about 32.58%; the corrosion rate of alternating stress conditions under alternating stress conditions is about 55.49%; Under the static stress, the corrosion rate of steel wire is somewhere in between, about 40.12%. Under stress-free condition, steel wire corrosion is more uniform, and the frequency of steel wire corrosion and corrosion rate is greater than the rest of the conditions, the degree of corrosion performance: Stress-free < static stress < alternating stress under stress-free condition.

Corrosion in the early stage, stress corrosion, and corrosion fatigue have little influence on tensile strength. In the middle and late stages of corrosion, the tensile strength began to decline sharply, the tensile strength of the steel wire appears briefly increased phenomenon under alternating stress and static stress conditions, and the ductility of steel wire decreased. In the late stages of corrosion, the alternating stress causes fatigue damage to the steel wire during the corrosion process, the toughness of the steel wire is significantly reduced, elongation after fracture of the steel wire is significantly lower than the other two loading states, at this time, the possibility of brittle fracture of the steel wire is high.

The stress of the steel wire bundle of the cable is in a dynamic redistribution process with the development of corrosion, and the cable will fracture rapidly when

the tensile force reaches the maximum bearing capacity. In order to ensure the safety of the cable in service, it is necessary to predict the crack expansion and the remaining service life of the cable in service based on the linear-elastic fracture mechanics, and to evaluate the safety performance of the existing damaged cable using different methods according to the actual project.

Acknowledgements

This chapter was supported by the National Natural Science Foundation of China (Grant No. 52178273), the Natural Science Foundation of Chongqing (Grant No. cstc2021jcyj-msxmX1159), the Chongqing Talent Plan Project (Grant No. cstc2022-ycjh-bgzxm0124), the Open Fund Project of State Key Laboratory of Mountain Bridge and Tunnel Engineering (Grant No. SKLBT-YF2105), the Chongqing Project of Joint Training Base Construction for Postgraduates (Grant No. JDLHPYJD2020004) and the Innovation Program for Graduate Student of Chongqing (Grant No. CYS22392 and 2021S0004).

Author details

Guowen Yao[1,2]*, Xuanbo He[1,2], Jiawei Liu[1,2], Jiangshan Lu[1,2] and Zengwei Guo[1,2]

1 School of Civil Engineering, Chongqing Jiaotong University, Chongqing, China

2 State Key Laboratory of Mountain Bridge and Tunnel Engineering, Chongqing Jiaotong University, Chongqing, China

*Address all correspondence to: yaoguowen@sina.com

References

[1] Yanaka Y, Kitagawa M. Maintenance of steel bridges on Honshu-shikoku crossing. Journal of Constructional Steel Research. 1982;**58**(1):131-150

[2] Barton SC, Carson CC, Gill RS. Implementation of pyrolysate analysis of materials employing tagging compounds to locate an overheated area in a generator. IEEE Transactions on Power Apparatus and Systems. 1982;**PER-1**(12): 4983-4989

[3] Kheyroddin A, Saghafi MH, Safakhah S. Strengthening of historical masonry buildings with fiber reinforced polymers (FRP). Advanced Materials Research. 2010;**133–134**:903-910

[4] Dolley EJ, Lee B, Wei RP. The effect of pitting corrosion on fatigue life. Fatigue and Fracture of Engineering Materials and Structures. 2000;**23**(7): 555-560

[5] Mahmoud KM. Fracture strength of a high strength steel bridge cable wire with a surface crack. Theoretical and Applied Fracture Mechanics. 2007; **48**(2):152-160

[6] Widyawati R, Takahashi J, Emoto H, Miyamoto A. Remaining life prediction of an aged bridge based on concrete core test. Procedia Engineering. 2014;**95**:88-99

[7] Mahmoud KM, Fisher JW. Mechanics of environment-assisted cracking in bridge cable wire. Bridge Structures. 2007;**3**:3-4

[8] Ou L, Gang S, Bo W, Chengxin Z. Inspection of technical condition of bridge stay cable in operation period. World Bridges. 2017;**45**(04):79-83

[9] Jun X, Weizhen C. Detection and analysis of the cable deterioration of Shimen bridge. Steel Construction. 2007; **05**:81-84

[10] Hailiang W, Jiafei X. Analysis of the cause of a bridge cable damage and suggestions. Railway Standard Design. 2005;**10**:67-69

[11] China Quality Inspection Press. Corrosion Tests in Artificial Atmospheres—Salt Spray Tests (GB/ T10125-1997). Beijing: China Quality Inspection Press; 1997

[12] Dongxia J. Experimental Study of Cable Environmental Corrosion Damage under Alternating Stress. Chongqing: Chongqing Jiaotong University; 2013

[13] Guowen Y, Shiya L, Zengwei G. Corrosion Fatigue Performance and Damage Mechanism of Bridge Cable Structures. Beijing: Science Press; 2022

[14] Li Z. Damage and Safety Performance Evaluation of the Cable-stayed Corrosion. Chongqing: Chongqing Jiaotong University; 2013

[15] Shicong Y. Research on the Corrosion-Fatigue Problems and Service Reliability of the Bridge Cables and Hangers. Chongqing: Chongqing Jiaotong University; 2018

[16] Shicong Y, Jinquan Z, Guowen Y. Microscopic damage behavior of corroded steel strands based on image gray analysis. Chinese Journal of Solid Mechanics. 2018;**39**(03):305-315

[17] Shicong Y, Guowen Y, Jinquan Z. Observations on the damage behaviors of corrosion fatigue in steel strands based on image analysis. Advances in Mechanical Engineering. 2017;**9**(12): 1-10

[18] China Standard Press. Hot-dip Galvanized Steel Wire for Bridge Cable (GB/T 17101-2008). Journal of Chongqing Jiaotong University (Natural Science). Beijing: China Standard Press; 2008

[19] Guowen Y, Chaoyue L, Guoqiang W. Mechanism of corrosion damage of stayed cable under the effect of acid rain and loading coupling. 2016;**35**(06):6-10

[20] Guowen Y, Xuesong C, Li Z. Study on corroded cable evaluation based on gray image analysis. Journal of Chongqing Jiaotong University (Natural Science). 2016;**35**(04):10-12

[21] Wenjie W. Experimental Study of Stay Cable Electrochemical Corrosion Fatigue under Alternating Stress State. Chongqing: Chongqing Jiaotong University; 2015

[22] Guoqiang W. Experimental study on Stress Corrosion and Corrosion Fatigue of Stay Cables under Acid Rain Condition. Chongqing: Chongqing Jiaotong University; 2015